

Scanning Electrochemical Microscopy. 40. Voltammetric Ion-Selective Micropipet Electrodes for Probing Ion Transfer at Bilayer Lipid Membranes

Shigeru Amemiya and Allen J. Bard*

Department of Chemistry and Biochemistry, The University of Texas at Austin, Austin, Texas 78712-1167

Voltammetric ion-selective micropipet electrodes for use in scanning electrochemical microscopy (SECM) for detection of potassium ion were fabricated. These used pulled borosilicate capillaries with tip orifice radii of 0.7–20 μm with silanized inner walls filled with a solution of 10 mM valinomycin and 10 mM ETH 500 in dichloroethane. The electrodes were characterized by determining the steady-state tip current for K^+ concentrations of 0.05–0.3 mM. The tips were used in the SECM feedback and generation–collection modes to study K^+ transfer through gramicidin channels in a horizontal bilayer lipid membrane (glycerol monooleate).

Scanning electrochemical microscopy (SECM) is a powerful technique to study charge (electron and ion) transfer at the solid/liquid interface,^{1,2} the gas/liquid interface,³ and the liquid/liquid interface.^{4,5} In most SECM experiments, the interfacial reactivity of an electrochemically active mediator is probed by studying the feedback effect, i.e., the change of the steady-state current that flows at the tip of a microelectrode positioned close to the interface.^{1,2} Recently, we have applied SECM to the extraction of kinetic information about ion-transfer (IT) reactions at planar bilayer lipid membranes (BLMs),⁶ where membrane permeability to conventional redox mediators was studied with a Pt disk microelectrode as the SECM tip. However, membrane permeability by electrochemically inactive ions, e.g., Na^+ , K^+ , Ca^{2+} , and Cl^- , is of biological interest because the transfer of these ions across BLMs is selectively mediated by channel-forming molecules, such as channel proteins and their peptide analogues.^{7,8}

In this paper, we describe the application of voltammetric ion-selective micropipet electrodes to the SECM studies of IT across BLMs. This approach allows for probing the channel-mediated transfer of electrochemically inactive ions across BLMs.

Although the charge-transfer processes across BLMs have been electrochemically studied because of their importance as model systems of biological membranes,⁹ a voltammetric microelectrode was applied only recently to the studies of BLMs by Matsue and co-workers.^{10,11} In their studies, Pt disk microelectrodes were positioned near BLMs to examine the permeability of unmodified BLMs¹⁰ or of alamethicin pores that were incorporated into BLMs as voltage-gated ion channels.¹¹ This technique allows for quantitatively probing the membrane permeability without the complication of the presence of unstirred layers near the membrane. More recently, we have shown that the SECM can be used to study the kinetics of charge-transfer processes at BLMs.^{5,6} Analysis of the SECM tip response demonstrates that unmodified BLMs behave as insulators to hydrophilic mediators, e.g., $\text{Ru}(\text{NH})_6^{3+}$ and $\text{Fe}(\text{CN})_6^{3-}$. The mediators were used to measure topographic images of BLMs surrounded by the annulus of organic solutions (the Plateau–Gibbs border). On the other hand, BLMs doped with I_2 showed some positive feedback with I^- as an electroactive mediator. Because most of the ion channels and their peptide analogues in BLMs selectively mediate the transfer of electrochemically inactive ions,^{7,8} a microelectrode that is sensitive to these ions is needed for SECM studies of IT across BLMs. *Potentiometric* ion-selective micropipet electrodes have been used to detect electrochemically inactive ions that are biologically important.¹² Indeed, Antonenko and co-workers have applied this technique to probe the concentration gradients of the solute ions that were induced within the unstirred layers adjacent to the BLMs.^{13–16} However, as shown in previous studies,^{17–20} the

- (1) Bard, A. J.; Fan, F.-R. F.; Mirkin, M. V. In *Electroanalytical Chemistry*; Bard, A. J., Ed.; Marcel Dekker: New York, 1993; Vol. 18, pp 243–373.
- (2) Bard, A. J.; Fan, F.-R. F.; Mirkin, M. V. In *Physical Electrochemistry: Principles, Methods and Applications*; Rubinstein, I., Ed.; Marcel Dekker: New York, 1995; pp 209–242.
- (3) Slevin, C. J.; Ryley, S.; Walton, D. J.; Unwin, P. R. *Langmuir* **1998**, *14*, 5331–5334.
- (4) Barker, A. L.; Gonsalves, M.; Macpherson, J. V.; Slevin, C. J.; Unwin, P. R. *Anal. Chim. Acta* **1999**, *385*, 223–240.
- (5) Amemiya, S.; Ding, Z.; Zhou, J.; Bard, A. J. *J. Electroanal. Chem.* **2000**, *483*, 7–17.
- (6) Tsionsky, M.; Zhou, J.; Amemiya, S.; Fan, F.-R. F.; Bard, A. J.; Dryfe, R. A. W. *Anal. Chem.* **1999**, *71*, 4300–4305.
- (7) Gennis, R. B. *Biomembranes: Molecular Structure and Function*; Springer-Verlag: New York, 1989.
- (8) *Single-Channel Recording*, 2nd ed.; Sakmann, B., Neher, E., Eds.; Plenum Press: New York, 1995.

- (9) Bender, C. J. *Chem. Soc. Rev.* **1988**, *17*, 317–346.
- (10) Yamada, H.; Matsue, T.; Uchida, I. *Biochem. Biophys. Res. Commun.* **1991**, *180*, 1330–1334.
- (11) Matsue, T.; Shiku, H.; Yamada, H.; Uchida, I. *J. Phys. Chem.* **1994**, *98*, 11001–11003.
- (12) Ammann, D. *Ion-Selective Microelectrodes*; Springer-Verlag: Berlin, 1986.
- (13) Antonenko, Y. N.; Bulychev, A. A. *Biochim. Biophys. Acta* **1991**, *1070*, 474–480.
- (14) Pohl, P.; Saparov, S. M.; Antonenko, Y. N. *Biophys. J.* **1997**, *72*, 1711–1718.
- (15) Antonenko, Y. N.; Pohl, P.; Denisov, G. A. *Biophys. J.* **1997**, *72*, 2187–2195.

response of potentiometric tips is not sensitive to the tip–membrane distance. Therefore, the distance had to be monitored by optical microscopy to avoid contact of the tip with the membrane,²¹ because the contact breaks the membrane and makes the tip response noisy and unstable.

We describe here the fabrication and application of *voltammetric* ion-selective micropipet electrodes to the SECM studies of IT reactions mediated by ion channels at BLMs. After introduction of micropipet electrodes to the studies of IT processes at the microinterface between two immiscible electrolyte solutions (“micro-ITIES”),^{22,23} SECM experiments using voltammetric micropipet electrodes were performed on the basis of the electron-transfer (ET)²⁴ and IT^{25–27} reactions across the micro-ITIES formed at the tip of the pipets. More recently, it was shown that silanization of the wall of glass micropipets allows for quantitative understanding of their voltammetric responses^{28–30} and SECM approach curves.²⁷ In this study, voltammetric K⁺-selective micropipet electrodes based on valinomycin were used to probe the K⁺ transfer through the pores of the ion channel-forming peptide gramicidin at BLMs. The geometry of the pipet electrodes was characterized by optical microscopy and by electrochemical techniques. The well-defined steady-state response of the pipet electrodes allows one to probe gramicidin-mediated K⁺ transfer across BLMs on the basis of the SECM feedback and generation–collection experiments.

EXPERIMENTAL SECTION

Chemicals. Valinomycin (Val) and tetradodecylammonium tetrakis(4-chlorophenyl)borate (ETH 500) from Fluka Chemika (Switzerland), gramicidin-*d* and glycerol monooleate from Sigma Chemical Co. (St. Louis, MO), chlorotrimethylsilane and *n*-decane from Aldrich (Milwaukee, WI), and 1,2-dichloroethane (DCE) from (EM Science, Gibbstown, NJ) were used as received. All aqueous solutions were prepared from deionized water (Milli-Q, Millipore Corp., Bedford, MA).

Fabrication of Ion-Selective Micropipet Electrodes. Micropipets were made from borosilicate capillaries (o.d./i.d. = 1.0/0.58 mm) from Sutter Instrument Co. (Novato, CA) using a laser-based pipet puller (model P-2000, Sutter Instrument). Prior to pulling, the glass capillaries were soaked in a 1:1 (v/v) mixture of concentrated sulfuric acid and 30% hydrogen peroxide overnight, washed thoroughly with deionized water, and dried at 120

°C for 30 min.¹⁸ The puller's five parameters (heat, filament, velocity, delay, and pull) were chosen to produce short (patch-clamp type) pipets. The program was found by trial and error and was modified as needed, because the performance of the puller changed slightly with time.³¹ Both the orifice radius and the thickness of the pipet wall were determined by optical microscopy and by electrochemical techniques.

The inner wall of each pipet was silanized to render it hydrophobic by filling it with a toluene solution of trimethylchlorosilane (5–100% v/v) from the larger opening.^{27–29} The solution was removed from the pipet with a syringe after 5–30 min. The silanized pipet was then connected to a vacuum pump to remove any remaining silanizing vapor inside the tip. The silanization time and the concentration of the silanization reagent were important, because unless its inner surface was sufficiently hydrophobic, the outer aqueous solution was drawn into the pipet.

A DCE solution of 10 mM valinomycin and 10 mM ETH 500 as ionophore and supporting electrolyte, respectively, was used to fabricate K⁺-selective micropipet electrodes. The very hydrophobic supporting electrolyte, ETH 500, was used in the organic phase to obtain a sufficiently wide potential window³² and also to avoid an ion-exchange reaction between K⁺ in the aqueous phase and the cationic electrolyte in the organic phase.³³ The silanized pipets were filled with the organic solution through the larger opening with a small (10 μ L) syringe. A 0.25-mm silver wire (Aldrich) was coated with silver tetrakis(4-chlorophenyl) borate (AgTPBCl) by reduction of Ag in a DCE solution of 10 mM tetrabutylammonium tetrakis(4-chlorophenyl) borate and was inserted into each pipet. The top of the pipet was then closed with Parafilm. The experimental system can be represented by the following cell



For all voltammetric and SECM experiments, a Pt wire was used as a counter electrode.

Electrochemical Cells for SECM Studies of BLMs. As opposed to conventional BLM apparatus, where the membrane is oriented vertically, the experiments described here utilized a horizontally oriented membrane that separated upper and lower compartments (Figure 1) for compatibility with the conventional SECM (model CHI 900, CH Instrument, Austin, TX).⁶ To prevent different pressures across the membrane, several holes (7-mm diameter) were made on the inner wall of the cell so that the pressures in the upper and lower compartments were the same. Silicone grease was used to seal the contacts between the O-rings and the Teflon partition (150- or 250- μ m thickness). A pinhole (~2-mm diameter) was made in the Teflon partition for the BLM. This type of cell allows the use of different solutions in the lower and upper compartments and allows the application of an external potential across the BLM. For the latter, a Ag/AgCl electrode was used as a substrate electrode, whose potential against the

(16) Pohl, P.; Saporov, S. M.; Antonenko, Y. N. *Biophys. J.* **1998**, *75*, 1403–1409.

(17) Horrocks, B. R.; Mirkin, M. V.; Pierce, D. T.; Bard, A. J.; Nagy, G.; Tóth, K. *Anal. Chem.* **1993**, *65*, 1213–1224.

(18) Wei, C.; Bard, A. J.; Nagy, G.; Tóth, K. *Anal. Chem.* **1995**, *67*, 1346–1356.

(19) Wei, C.; Bard, A. J.; Kapui, I.; Nagy, G.; Tóth, K. *Anal. Chem.* **1996**, *68*, 2651–2655.

(20) Kashyap, R.; Gratzl, M. *Anal. Chem.* **1999**, *71*, 2814–2820.

(21) Tripathi, S.; Hladky, S. B. *Biophys. J.* **1998**, *74*, 2912–2917.

(22) Taylor, G.; Girault, H. H. *J. Electroanal. Chem.* **1986**, *208*, 179–183.

(23) Ohkouchi, T.; Kakutani, T.; Osakai, T.; Senda, M. *Anal. Sci.* **1991**, *7*, 371–376.

(24) Solomon, T.; Bard, A. J. *Anal. Chem.* **1995**, *67*, 2787–2790.

(25) Solomon, T.; Bard, A. J. *Bull. Chem. Soc. Ethiop.* **1997**, *11*, 55–59.

(26) Shao, Y.; Mirkin, M. V. *J. Electroanal. Chem.* **1997**, *439*, 137–143.

(27) Shao, Y.; Mirkin, M. V. *J. Phys. Chem. B* **1998**, *102*, 9915–9921.

(28) Shao, Y.; Mirkin, M. V. *Anal. Chem.* **1998**, *70*, 3155–3161.

(29) Horrocks, B. R.; Mirkin, M. V. *Anal. Chem.* **1998**, *70*, 4653–4660.

(30) Liao, Y.; Okuwaki, M.; Kitamura, F.; Ohsaka, T.; Tokuda, K. *Electrochim. Acta* **1998**, *44*, 117–124.

(31) Liu, B.; Shao, Y.; Mirkin, M. V. *Anal. Chem.* **2000**, *72*, 510–519.

(32) Jadhav, S.; Bakker, E. *Anal. Chem.* **1999**, *71*, 3657–3664.

(33) Koryta, J.; Kozlov, Y. N.; Skalic, M. *J. Electroanal. Chem.* **1987**, *234*, 355–360.

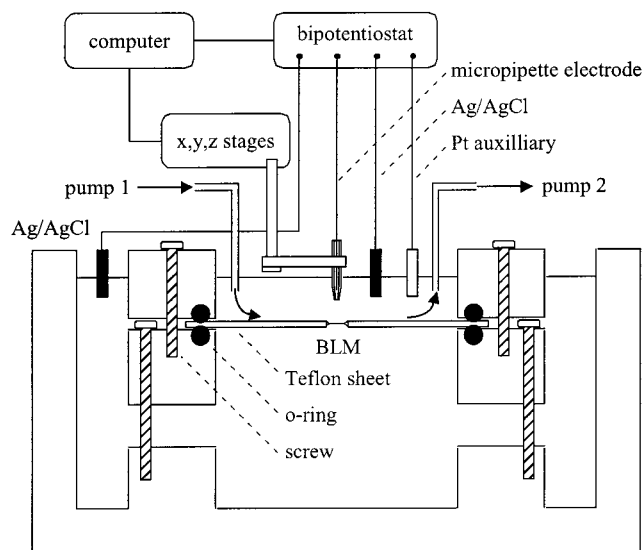


Figure 1. Schematic diagram of SECM apparatus and a cell for the preparation of horizontally oriented BLM.

reference electrode in the upper compartment was controlled by the bipotentiostat in the SECM apparatus. For experiments with different solutions in the lower and upper compartments, a dual HPLC pump (model AA-100-S-PK, Eldex, Napa, CA) was used. After the formation of the BLM between the lower and upper compartments containing the same solution, the original solution in the upper compartment was removed with one of the pumps (pump 2 in Figure 1) and a new solution was simultaneously introduced with the other pump (pump 1). The same flow rate was employed for the two pumps by careful adjustment to prevent different pressures across the membrane. The completion of the exchange was checked by measuring the analyte concentration with a micropipette electrode.

BLMs were prepared from 10 mg/mL lipid solutions in *n*-decane by the standard brush technique.³⁴ For the preparation of gramicidin-incorporated BLMs, aqueous gramicidin solutions, obtained by dilution of 0.1 mM gramicidin in ethanol with the aqueous solution of supporting electrolyte, were used in both compartments of the electrochemical cell. Formation of the BLM was monitored using a color CCD camera (TK-C1380, JVC, Japan), mounted on a microscope (LDM-1/s, KATOPTARon) to detect the interference fringes caused by the thinning of the organic layer.³⁵ A neutral lipid, glycerol monooleate, which has been frequently used for studies of gramicidin-mediated IT at BLMs,^{36,37} was used for all BLM experiments. Note that, in preliminary experiments, the K^+ -selective micropipette electrodes did not show clear voltammograms in the aqueous solution containing phospholipids. This is probably caused by the valinomycin-mediated K^+ transfer at the micro-ITIES being inhibited by the adsorption of the lipids.³⁸

(34) Hanke, W.; Schlue, W. *Planar Lipid Bilayers: Methods and Applications*; Academic Press: London, New York, 1993.

(35) Tien, H. T. *Bilayer Lipid Membranes (BLM): Theory and Practice*; Marcel Dekker: New York, 1978.

(36) Hladky, S. B.; Haydon, D. A. *Curr. Top. Membr. Transport* **1984**, *21*, 327–372.

(37) Woolley, G. A.; Wallace, B. A. *J. Membr. Biol.* **1992**, *129*, 109–136.

(38) Chesniuk, S. G.; Dassie, S. A.; Yudi, L. M.; Baruzzi, A. M. *Langmuir* **1998**, *14*, 5226–5230.

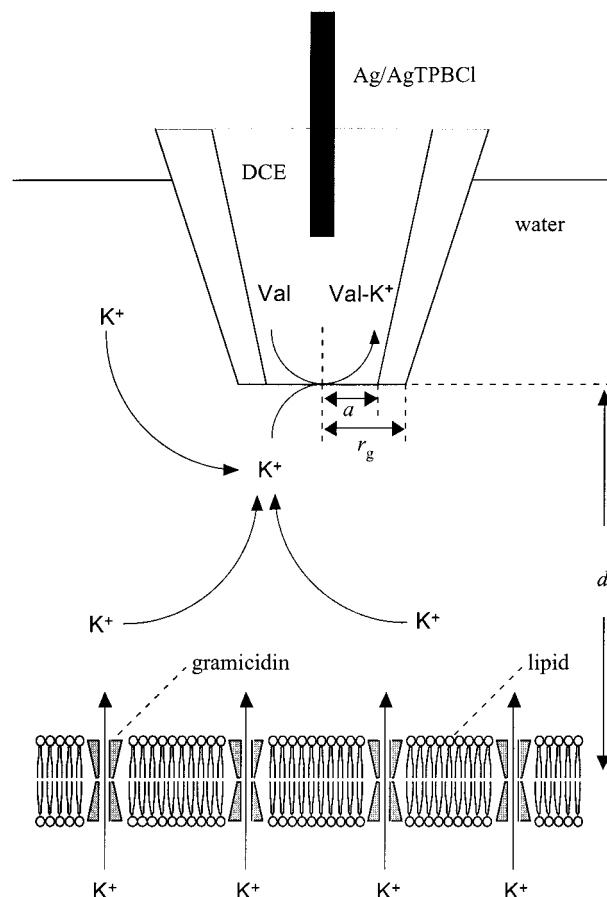
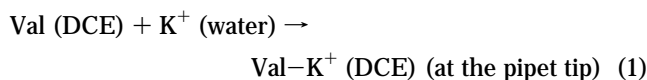


Figure 2. Schematic diagram of the voltammetric responses and SECM experiments at a BLM using a K^+ -selective micropipette electrode based on valinomycin. The micropipette electrode is characterized by the electrode radius, a , and r_g is the distance from the center to the edge of the pipet. The BLM is located at the distance d .

RESULTS AND DISCUSSION

Voltammetric and SECM Characterization of Micropipette Electrodes. A K^+ -selective micropipette electrode based on valinomycin was used to probe the channel-mediated transfer of the ion across the BLM. Because of the high selectivity in the complexation of valinomycin with K^+ , valinomycin selectively assists interfacial K^+ transfer in the presence of the aqueous supporting electrolytes that are necessary for obtaining stable BLMs. Although the valinomycin-facilitated K^+ transfer has previously been studied at a large ITIES,^{33,38} there have been no reports on the reaction at a water/DCE microinterface. Thus, K^+ -selective micropipette electrodes of different radii (0.7–20 μm) were characterized on the basis of voltammetric and SECM experiments.

At the water/DCE interface formed at the tip of the micropipette electrode (cell 1), the facilitated IT reaction occurs as follows (Figure 2 without BLMs)



The micro-ITIES at the pipet tip is polarizable, and the voltage, ΔE , applied between the Ag/AgTPBCl electrode inside the pipet and the Ag/AgCl electrode in the aqueous phase provides the

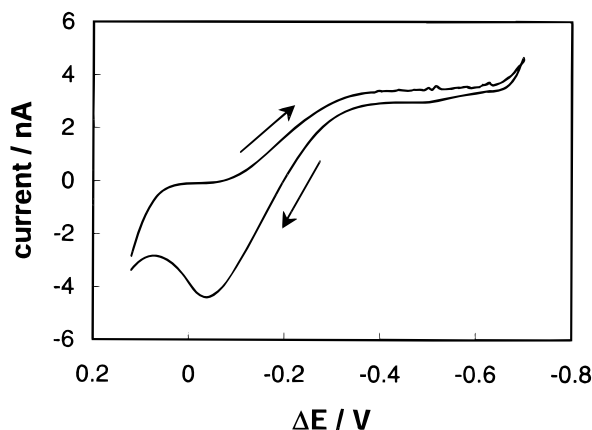


Figure 3. Cyclic voltammogram of valinomycin-mediated K^+ transfer across the water/DCE interface formed at the tip of a $20\text{-}\mu\text{m}$ -radius micropipet. The potential sweep rate was 20 mV/s . The aqueous phase contained 0.2 mM KCl and 10 mM MgSO_4 . For other parameters, see cell 1 in the text.

driving force for the IT process. Figure 3 shows the voltammogram for K^+ transfer as obtained with a $20\text{-}\mu\text{m}$ -radius pipet electrode. The upper part of the curve in Figure 3 (forward scan) represents K^+ transfer from water to DCE inside the pipet. With the pipet biased at a sufficiently negative potential, a steady-state current was obtained. This result indicates that the current is limited by spherical diffusion of K^+ in the outer aqueous phase to the pipet orifice (as seen with amperometric ultramicroelectrodes). During the reverse potential scan, a peaked non-steady-state voltammogram was obtained for the dissociation of the valinomycin- K^+ complexes at the micro-ITIES. This indicates that the current here is limited by essentially linear diffusion of the valinomycin- K^+ complex in a narrow shaft of the pipet. Analysis of the forward scan in voltammograms for micropipets with different radii ($0.7\text{--}20\text{ }\mu\text{m}$) showed that the valinomycin-assisted K^+ transfer appeared quasi-reversible (Figure 3).³⁹ This is not caused only by the iR drop in the organic phase because the voltammogram after iR drop compensation ($R = 10\text{ M}\Omega$) is still quasi-reversible. Indeed, a small electrode ($a = 0.7\text{ }\mu\text{m}$) showed slightly more reversible voltammograms than a larger electrode ($a = 20\text{ }\mu\text{m}$). It is unlikely that this quasi-reversibility represents actual kinetic limitations in K^+ transfer or reaction with valinomycin. Other reasons for the apparent quasireversibility, such as some potential-dependent irregularities of the ITIES,⁴⁰ cannot be excluded.

In SECM experiments, a steady-state tip current is required. For the K^+ -selective micropipet electrodes, this steady-state current is obtained only when the concentration of valinomycin is much higher than the K^+ concentration. Thus, voltammograms with different K^+ concentrations were measured to determine the K^+ concentration range where a steady-state current was found. When the K^+ concentration was varied from 0.05 to 0.3 mM , a steady-state current was obtained with a $10\text{-}\mu\text{m}$ -radius micropipet electrode (Figure 4). However, at higher concentrations, the voltammogram was slightly peaked, indicating that the current was affected by the quasi-linear diffusion of free valinomycin in a narrow shaft of the pipet. When the concentration of valinomycin

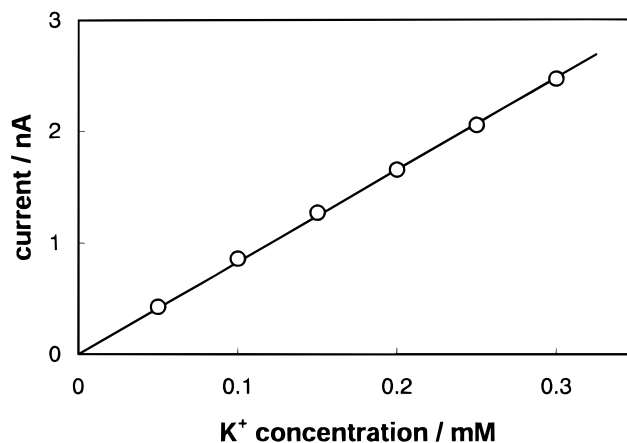


Figure 4. K^+ concentration dependence of the steady-state current for valinomycin-assisted K^+ transfer across the water/DCE interface formed at the tip of a $10\text{-}\mu\text{m}$ -radius micropipet. The potential sweep rate was 20 mV/s . The aqueous phase contained $0.05\text{--}0.3\text{ mM KCl}$ and 10 mM MgSO_4 . For other parameters, see cell 1 in the text.

is much higher than that of K^+ , the limiting current, $i_{T,\infty}$, as observed on the forward scan in Figure 3, can be expressed by the following equation^{27,28}

$$i_{T,\infty} = \text{const}FaDc \quad (2)$$

where F is Faraday's constant, D is the diffusion coefficient of the transferred ion, c is its bulk concentration, a is the inner radius of the tip, and const is a value that depends on the shape of the micro-ITIES and on the insulator geometry of the tip. Assuming a disk-shaped ITIES with $RG = 1.5$ ($RG = r_g/a$, where r_g is the radius of the glass insulator of the tip), eq 2 with $\text{const} = 4.64$ ²⁷ and $D = 1.95 \times 10^{-5}\text{ cm}^2/\text{s}$ gave $a = 9.4\text{ }\mu\text{m}$. The RG and a agree with those values estimated by optical microscopy. Furthermore, Figure 4 implies that the maximum tip current that is not affected by the diffusion of valinomycin inside the pipet is $\sim 2.5\text{ nA}$ for a $10\text{-}\mu\text{m}$ -radius tip. This maximum current depends on the concentration of valinomycin and on the geometry of the micropipet tip. Thus, in all of the following SECM experiments, tip currents that are less than the maximum current were used. This allowed the use of the SECM theories developed for micropipet electrodes.²⁷

By optimization of the parameters of the pipet puller, smaller tips, with radii less than $1\text{ }\mu\text{m}$, could be obtained. However, such pipets are too small to estimate the tip geometry (i.e., RG and a) by optical microscopy. Thus, the tip geometry was characterized on the basis of the SECM feedback experiments using a Teflon sheet as an insulating substrate. Figure 5 shows an approach curve obtained with a $0.7\text{-}\mu\text{m}$ -radius pipet tip. As the tip approached the Teflon sheet, the tip current decreased because the diffusion of K^+ to the pipet orifice was hindered by the Teflon sheet. The experimental approach curve was analyzed on the basis of the following SECM equation for insulating substrates calculated for electrodes with $RG = 1.5$ ²⁷

$$\frac{i_T}{i_{T,\infty}} = \frac{1}{1.0035959 + \frac{0.9294275}{d/a} + 0.4022603 \exp\left(-\frac{1.788572}{d/a}\right) + \frac{0.2832628d/a}{d/a + 0.1401598}} \quad (3)$$

(39) Mirkin, M. V.; Bard, A. J. *Anal. Chem.* **1992**, *64*, 2293–2302.

(40) Kakiuchi, T. *Electrochem. Commun.* **2000**, *2*, 317–321.

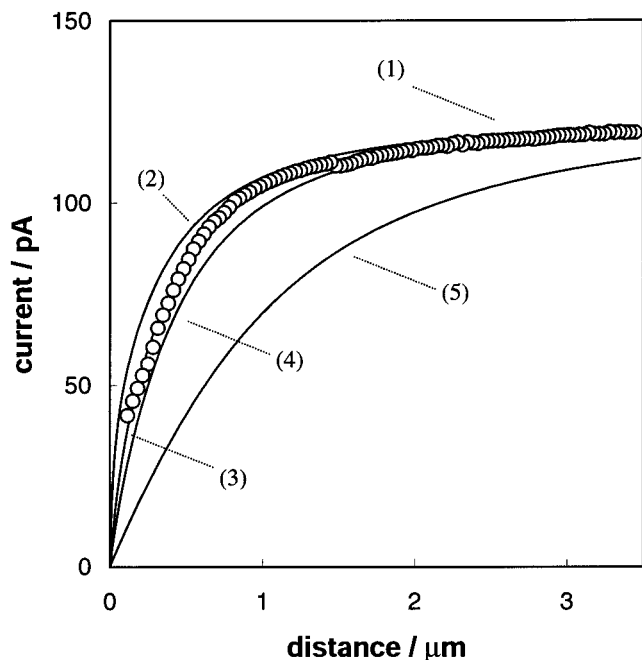


Figure 5. Current–distance curve with a Teflon sheet substrate as obtained with a K^+ -selective micropipet electrode based on valinomycin (curve 1) and numerical simulations with different parameters (curves 2–5). The tip was scanned at $1 \mu\text{m/s}$. The aqueous phase contained 0.2 mM KCl and 10 mM MgSO_4 . The solid lines represent SECM theory for an insulating substrate. RG and a (μm): (2) 1.1 and 0.64; (3) 1.5 and 0.71 (eq 3); (4) 2.0 and 0.75; (5) 10 and 0.83. For theoretical equations of curves 2, 4, and 5, see ref 27.

where d is the distance between the tip and substrate. Equation 3, which was originally derived on the basis of the numerical simulation by Shao and Mirkin,²⁷ agrees well with the results of finite element method⁴¹ and boundary element method.⁴² As shown in Figure 5, the experimental approach curve fits eq 3 much better than a theoretical curve for $RG = 10$ and also slightly better than the theoretical curves for $RG = 1.1$ and 2.0 . The analysis gives $a = 0.71 \mu\text{m}$ and shows that the closest distance attained between the tip and the Teflon sheet was only 115 nm . The closest tip/substrate distance is equivalent to the normalized distance of 0.16 , which is much smaller than the closest normalized distances that were obtained at a Teflon sheet with larger micropipets ($a > 10 \mu\text{m}$). This is probably because the tip of the small pipet is smoother than that of the larger pipets.⁴³ Note that electrochemical and optical microscopic analysis of all electrodes developed in this study gave $RG = 1.5$, although micropipet electrodes with $RG = 1.1$ were reported previously.²⁷ This difference in RG values may be due to the different parameters used for the pipet puller, suggesting the importance of careful characterization of the pipet geometries.

SECM Feedback Based on Gramicidin-Mediated K^+ Transfer across the BLM. To check the applicability of the K^+ -selective micropipet electrodes to the SECM studies of the channel-mediated IT across the BLM, feedback experiments were per-

formed for BLMs containing gramicidin as an ion channel-forming peptide (Figure 2). In these experiments, a K^+ concentration gradient across BLMs was used as the driving force for K^+ transfer. Gramicidin-incorporated BLMs were formed in the following cell

upper compartment : $0.2 \text{ mM KCl} + 10 \text{ mM MgSO}_4 + 0.5 \mu\text{M gramicidin}$	(cell 2)
BLM	
lower compartment : $x \text{ mM KCl} + 10 \text{ mM MgSO}_4 + 0.5 \mu\text{M gramicidin}$	

In contrast to unmodified BLMs, gramicidin-incorporated BLMs are highly conductive because gramicidin molecules dimerize in the BLMs to form pores.^{36,37} The pores are permeable to alkali metal ions but not to inorganic anions. Furthermore, gramicidin channels are impermeable to alkaline earth metal ions and can be blocked by these ions, although the blocking effect of Mg^{2+} is much smaller than that of Ca^{2+} and Ba^{2+} .⁴⁴ Thus, in cell 2, K^+ is the only permeable ion, and the K^+ concentration difference between the upper and lower compartments is kept at equilibrium and is energetically compensated by the generation of a membrane potential.⁴⁵ As a micropipet tip in the upper compartment approached the BLM, the K^+ concentration in the compartment near the membrane was depleted because of K^+ transfer from the aqueous phase into the organic filling solution inside the pipet (eq 1). This depletion induces the K^+ transfer across the BLM from the lower to the upper compartment



The flux, which reflects the dynamics of the K^+ transfer, can be detected as a feedback effect on the steady-state current of the micropipet tip. This experiment is similar to SECM-induced transfer experiments, which were described theoretically by Unwin's group^{46–48} and were applied to BLM studies.^{6,10}

Figure 6a shows approach curves obtained with a $10\text{-}\mu\text{m}$ -radius pipet tip with and without a K^+ concentration gradient across the BLM ($x = 0.2$ and 10 , respectively, in cell 2). Without a concentration gradient across the BLM, the tip current decreased from its transport-limited current at large d , $i_{T,\infty}$, as the BLM was approached (curve 1). This current decrease is due to hindered diffusion of K^+ toward the tip caused by the presence of the BLM. When the tip made contact with the BLM, the bilayer broke and the tip current, after a transient, returned to the $i_{T,\infty}$ value once more. A similar phenomenon was previously seen with conventional Pt microelectrode tips.⁶ The declining portion of the approach curve was compared with the theoretical curve obtained by assuming purely negative feedback (Figure 6b, curve 1). The shape of the experimental BLM approach curve was very similar to that of the theoretical approach curve (eq 3) for $RG = 1.5$ and $a = 10.3 \mu\text{m}$, which are consistent with those observed by optical microscopy. Thus, the two curves essentially superimpose when the position corresponding to $d = 0$ from the experimental data

(44) Bamberg, E.; Luger, P. *J. Membr. Biol.* **1977**, *35*, 351–375.

(45) Myers, V. B.; Haydon, D. A. *Biochim. Biophys. Acta* **1972**, *274*, 313–322.

(46) Slevin, C. J.; Umbers, J. A.; Atherton, J. H.; Unwin, P. R. *J. Chem. Soc., Faraday Trans.* **1996**, *92*, 5177–5180.

(47) Slevin, C. J.; Macpherson, J. V.; Unwin, P. R. *J. Phys. Chem. B* **1997**, *101*, 10851–10859.

(48) Barker, A. L.; Macpherson, J. V.; Slevin, C. J.; Unwin, P. R. *J. Phys. Chem. B* **1998**, *102*, 1586–1598.

(41) Amphlett, J. L.; Denuault, G. *J. Phys. Chem. B* **1998**, *102*, 9946–9951.

(42) Fulian, Q.; Fisher, A. C.; Denuault, G. *J. Phys. Chem. B* **1999**, *103*, 4393–4398.

(43) Brown, K. T.; Flaming, D. G. *Advanced Micropipette Techniques for Cell Physiology*; Wiley: New York, 1986.

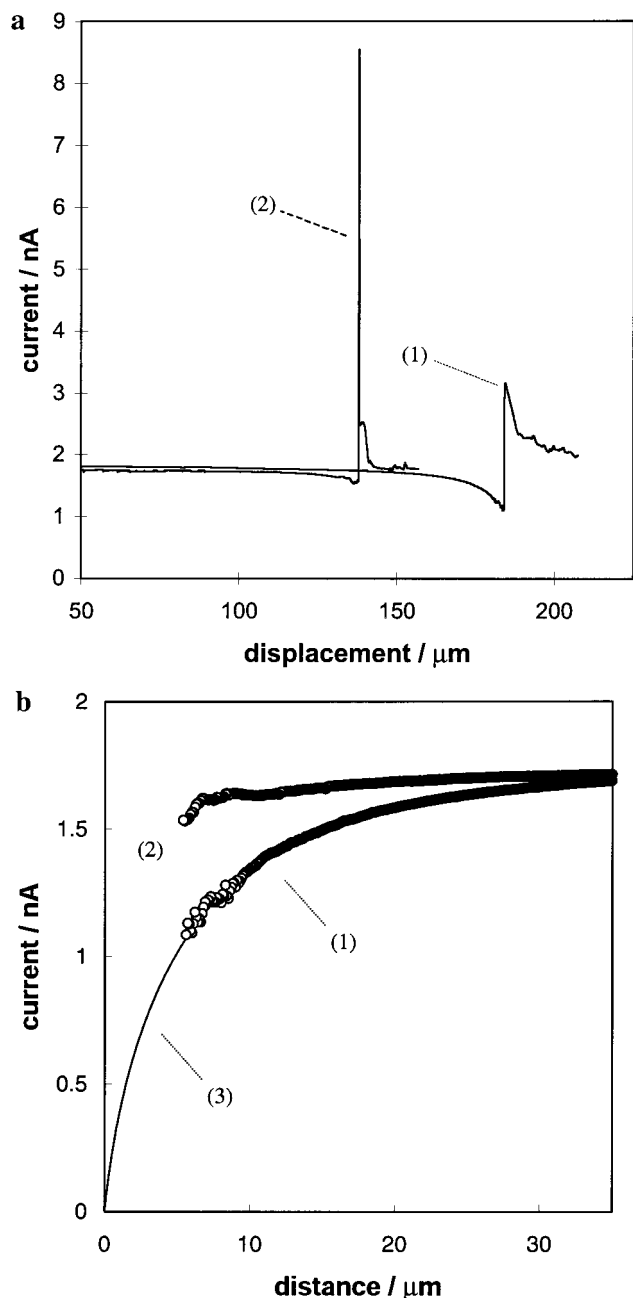


Figure 6. (a) Approach curves of a BLM incorporating gramicidin channels as obtained with a K^+ -selective micropipet electrode based on valinomycin. The aqueous phase in the lower compartment contained 10 mM $MgCl_2$ and 0.2 mM KCl (curve 1) or 10 mM KCl (curve 2). The tip was scanned at $3 \mu m/s$. For other parameters, see cells 1 and 2 in the text. (b) Analysis of the experimental approach curves in (a). The solid line (curve 3) represents SECM theory for an insulating substrate with $RG = 1.5$ and $a = 10.3 \mu m$ (eq 3). The distance for curve 2 was arbitrarily adjusted so that the closest distance between the tip and BLM is the same as that for curve 1.

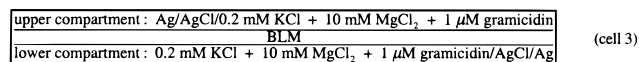
was empirically adjusted. Although the conductivity of the BLM incorporating gramicidin channels is small, but finite, this result indicates that K^+ transfer across the BLM is very slow without a K^+ concentration gradient.⁴⁹ Additionally, Figure 6b shows that the BLM was broken when the opening in the tip was $\sim 5 \mu m$ from

(49) Bard, A. J.; Mirkin, M. V.; Unwin, P. R.; Wipf, D. O. *J. Phys. Chem.* **1992**, *96*, 1861–1868.

the membrane. Similar phenomena were previously observed with $12.5\text{-}\mu m$ -radius Pt microelectrodes and were attributed to the glass sheath of the electrodes touching the membrane because of some tilting in the alignment between the tip and bilayer.⁶ Although the glass sheath of the micropipet electrodes ($RG = 1.5$) is much thinner than that of the Pt microelectrodes ($RG = 4\text{--}10$), the tips of the micropipet electrodes are much rougher than those of the Pt microelectrodes with a similar electrode radius, as observed by optical microscopy. The combination of the tip roughness and the tilted tip/membrane alignment makes it difficult for the pipet tip to approach the membrane to very small d values.

On the other hand, a different behavior was observed when the lower compartment contained a K^+ solution of a higher concentration ($x = 10$ in cell 2). When the tip was far from the membrane, the tip current was nearly identical to that obtained without the concentration gradient across the BLM. This result indicates that the original K^+ solution (10 mM) in the upper compartment was replaced with the 0.2 mM K^+ solution. As the tip approached the membrane, the tip current decreased to 85% of $i_{T,\infty}$ (Figure 6a, curve 2). This decrease in the current was much smaller than that observed without a concentration gradient (Figure 6b). This can be explained as follows. A higher K^+ concentration in the lower compartment increases the driving force for K^+ transfer from the lower to upper compartment. This resulted in an increase of the feedback effect on the steady-state current of the micropipet tip. As the pipet further approached the BLM, the tip current suddenly increased and then decayed, because of contact of the tip with the 10 mM K^+ solution after the membrane was broken. Note that the interpretation of the magnitude of the tip current after contact with the 10 mM K^+ solution is complicated, because under these conditions, the tip current is based on the quasi-linear diffusion of free valinomycin in a narrow shaft of the pipet. We attempted a numerical simulation for the approach curve with a concentration gradient using the PDEase2 program package.⁵⁰ However, the experimental approach curve did not fit well with theoretical curves based on the simplified assumption that the K^+ transfer across the BLM (eq 4) can be represented by a first-order interfacial rate constant. More detailed studies are necessary to understand quantitatively the dynamics of the K^+ transfer.

Probing K^+ Concentration Profiles near BLMs. In the previous section, a concentration gradient across the BLM was used as the driving force for K^+ transfer. In this section, an externally applied potential across the BLM was used as the driving force. The experiments were performed in the following cell



In this cell, when a positive potential was applied to the $Ag/AgCl$ electrode in the lower compartment versus the reference electrode in the upper compartment, K^+ transfer was induced from the lower to the upper compartment. The K^+ concentration profiles in the upper compartment near the BLM were probed with a K^+ -selective micropipet electrode. Simultaneously, the K^+ flux across

(50) Mirkin, M. V. In *Scanning Electrochemical Microscopy*; Bard, A. J., Mirkin, M. V., Eds.; Marcel Dekker: New York, in press.

the BLM was detected as the membrane current between the Ag/AgCl electrodes. This experiment is analogous to an SECM generation–collection experiment^{1,2} as K^+ generated at the BLM is collected at the micropipet tip. The radius of the pipet was so small ($\sim 1 \mu\text{m}$) that the tip current was not affected by the feedback effect until the tip was approached to less than several micrometers from the membrane. Because the K^+ transfer is activated by a potential difference across the BLM, the membrane potential, E_{mem} , was defined as follows

$$E_{\text{mem}} = E_{\text{app}} - E_{\text{eq}} \quad (5)$$

where E_{app} is the potential applied to the Ag/AgCl electrode in the lower compartment and E_{eq} is the equilibrium potential measured with the same electrode.

To determine the initial position of the BLM, an approach curve was measured without an applied potential (curve 1 in Figure 7a). The $1\text{-}\mu\text{m}$ -radius micropipet tip was then moved toward the membrane until the tip current decreased to 85% of $i_{T,\infty}$. The approach curve fits the theoretical curve for an insulating substrate (eq 3) very well, indicating that K^+ transfer across the gramicidin-incorporated BLM was quite slow and is consistent with results obtained with a larger electrode (curves 1 in Figure 6a and b). The analysis gave the inner radius of the tip, $a = 1.1 \mu\text{m}$, and $RG = 1.5$. The micropipet was then withdrawn by $100 \mu\text{m}$ from the position where the tip current decreased to 85% of $i_{T,\infty}$ ($2.4 \mu\text{m}$ from the membrane). A membrane potential of 110 mV was applied for 40 s until the current flowing through the BLM (the membrane current, i_{mem}) became nearly constant. The tip current increased as the micropipet approached the BLM under the applied membrane potential (Figure 7a). Because the tip current is proportional to the local K^+ concentration near the tip (eq 2), the increase of the tip current indicates that K^+ ions have accumulated near the membrane to cause an increase in the concentration. When the pipet was very close to the BLM, the tip current decreased, because the diffusion of K^+ to the tip was hindered by the BLM. The onset of this negative feedback allowed us to avoid breakage of the membrane, which is characterized by a sharp increase in the tip current (for example, see Figure 6a) and also in the membrane current. Thus, at this point, the pipet was stopped and withdrawn by $100 \mu\text{m}$. An analogous experiment was then performed with $E_{\text{mem}} = 60 \text{ mV}$. As the tip approached the BLM, the tip current increased gradually and then decreased. As expected, the tip current in curve 3 was smaller than that in curve 2 ($E_{\text{mem}} = 110 \text{ mV}$) but was still much higher than that in curve 1 ($E_{\text{mem}} = 0 \text{ mV}$). Finally, a similar experiment was performed with $E_{\text{mem}} = 160 \text{ mV}$. The tip current in curve 4 was larger than that in curves 1–3. In these experiments, no evidence of membrane breakage was observed either in the tip current or in the membrane current. This result confirms that all of the approach curves 1–4 were measured with the same BLM. Note that the distance at which the tip current began to decrease was $\sim 8 \mu\text{m}$ larger for curves 3 and 4 than for curves 1 and 2. The decrease of the tip current is due to the feedback effect, which can be observed only when the distance between the tip and substrate is smaller than a few times by the tip radius. Because the tip radius is $1.1 \mu\text{m}$ in this experiment, the difference of $8 \mu\text{m}$ cannot be ascribed only to a different degree of the feedback effect.

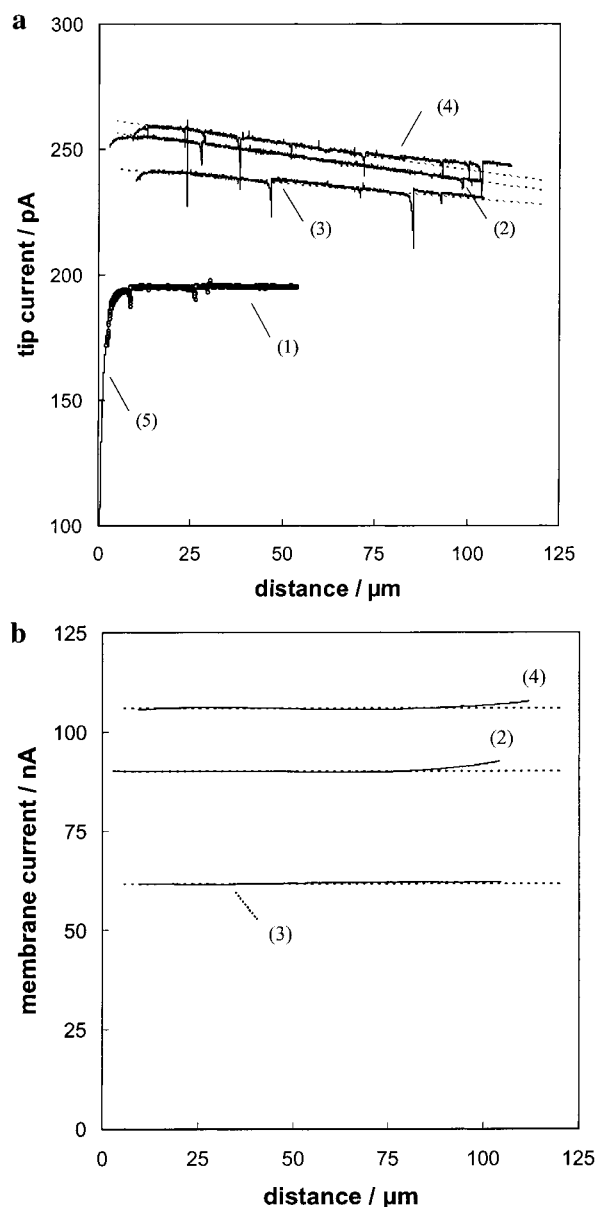


Figure 7. (a) Current–distance curves of a BLM incorporating gramicidin channels as obtained with a K^+ -selective micropipet electrode based on valinomycin and (b) simultaneously measured membrane currents. The membrane potential was 0, 110, 60, and 160 mV for the respective curves 1–4. The tip was scanned at $1 \mu\text{m/s}$. For other parameters, see cells 1 and 3 in the text. Curve 5 in (a) represents SECM theory for an insulating substrate with $RG = 1.5$ and $a = 1.13 \mu\text{m}$ (eq 3). The dotted lines in (a) were obtained by a linear fit of the respective current–distance curves in the range of $20 < d (\mu\text{m}) < 70$ (eq 9). The average of the membrane current in the range of $20 < d (\mu\text{m}) < 70$ is plotted as the dotted line in (b).

Probably, the difference is due to an irreversible change in the position of the BLM between the scan at 110 mV and that at 60 mV . Indeed, applied membrane potentials are known to induce a thinning of a BLM, as well as a change in the shape of the membrane and surrounding annulus.⁵¹

The gramicidin-incorporated BLMs can be regarded as an array of small active sites (gramicidin pore, $\sim 4\text{-}\text{\AA}$ diameter³⁶) on

(51) Picard, G.; Denicourt, N.; Fendler, J. H. *J. Phys. Chem.* **1991**, *95*, 3705–3715.

Table 1. Influence of Membrane Potentials on K⁺ Concentration Profiles near BLMs As Probed with K⁺-Selective Micropipet Electrodes Based on Valinomycin

	E_{mem} (mV)		
	60	110	160
m^a (nA·mm ⁻¹)	-0.122	-0.197	-0.205
b^a (pA)	243	258	263
j_{mem}^b (nA·mm ⁻²)	23	37	39
i_{mem}^c (nA)	61.7	90.1	106
R_{mem}^d (mm)	0.91	0.86	0.92

^a Obtained by fitting the tip current with eq 9 in the range of $20 < x$ (μm) < 70 . ^b Calculated with eq 10 using $a = 1.1 \mu\text{m}$ and the values of m in this table. ^c The average of the membrane current in the range $20 < x$ (μm) < 70 . ^d Calculated on the basis of eq 12.

a large insulating substrate (BLM, 1–2-mm diameter). Each gramicidin pore is small enough to achieve a steady-state K⁺ flux through the pore within a very short time.⁵² However, the overlap of the diffusion layers of adjacent pores will produce a macroscopic total current across the substrate.⁵³ In the cases represented by curves 2–4 in Figure 7b, the membrane currents were almost constant with time after 40 s. The following analysis was performed on the basis of a quasi-steady-state membrane current. All the parameters obtained from this analysis are given in Table 1.

Because a BLM is a large planar substrate, Fick's first law gives the membrane current density, j_{mem} ,⁵⁴ at the tip location, x , as

$$j_{\text{mem}} = -FD(\partial c_{\text{K}^+}(x)/\partial x) \quad (6)$$

where x is the distance from the membrane and $c_{\text{K}^+}(x)$ is the local K⁺ concentration at x . When the tip is positioned sufficiently far from the membrane that there is no SECM feedback effect, the steady-state tip current, $i_{\text{T}}(x)$, is proportional to the local K⁺ concentration; on the basis of eq 2 we can write

$$i_{\text{T}}(x) = 4.64FaDc_{\text{K}^+}(x) \quad (7)$$

The combination of eqs 6 and 7 relates j_{mem} and i_{T}

$$j_{\text{mem}} = -\frac{1}{4.64a} \frac{\partial i_{\text{T}}(x)}{\partial x} \quad (8)$$

Furthermore, in this region a linear dependence of the tip current on the tip–membrane distance is observed (Figure 7a). Thus, in the range of $20 < x$ (μm) < 70 , current–distance curves 2–4 in Figure 7a can be fit to the following equation

$$i_{\text{T}}(x) = mx + b \quad (9)$$

(52) Andersen, O. S.; Feldberg, S. W. *J. Phys. Chem.* **1996**, *100*, 4622–4629.

(53) Forouzan, F.; Bard, A. J.; Mirkin, M. V. *Isr. J. Chem.* **1997**, *37*, 155–163.

(54) Bard, A. J.; Faulkner, L. R. *Electrochemical Methods: Fundamentals and Applications*; John Wiley & Sons: New York, 1980.

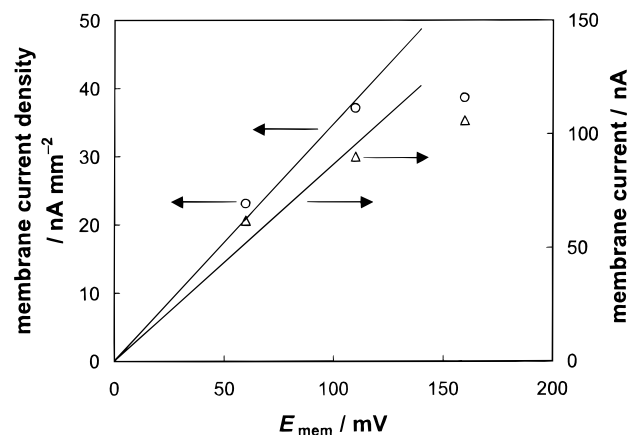


Figure 8. Potential dependence of the membrane current density (O) and of the membrane current (Δ) as calculated from the current–distance curves 2–4 in Figure 7a and b, respectively. The membrane current density was calculated on the basis of eq 10. The membrane current is the average value that is represented with the dotted lines in Figure 7b. For details, see text and Table 1.

Thus, from eq 8

$$j_{\text{mem}} = -(m/4.64a) \quad (10)$$

The membrane current density was calculated on the basis of eq 10 using $a = 1.1 \mu\text{m}$ and the respective value of m for curves 2–4. A plot of the membrane current density versus the membrane potential is shown in Figure 8. The current density was proportional to the potential when $0 \leq E_{\text{mem}}$ (mV) ≤ 110 . This result indicates that the gramicidin-incorporated BLM behaves as a resistance in this potential range. When $E_{\text{mem}} = 160$ mV, the current density was nearly the same as that with $E_{\text{mem}} = 110$ mV. This can be explained as follows. There are at least three steps in the K⁺-transfer reaction across the gramicidin-incorporated BLM, i.e., diffusion of K⁺ from the bulk aqueous phase to proximity to a gramicidin pore, K⁺ transfer across the pore, and diffusion of K⁺ from the pore proximity to the bulk aqueous phase. Among these processes, only the transfer process is expected to be potential dependent. When the K⁺ transfer across the gramicidin pore is activated with sufficiently large membrane potentials, the membrane current becomes limited by the diffusion of K⁺, which is potential independent.

In the previous paragraph, the membrane current density was calculated from the current–distance curve as obtained with the micropipet electrode. Here, the current density is compared with the total membrane current on the basis of the following equation

$$i_{\text{mem}} = A_{\text{mem}}j_{\text{mem}} \quad (11)$$

where A_{mem} is the membrane area. A plot of the membrane current versus the membrane potential is shown in Figure 8. The membrane currents are a slight function of tip position (Figure 7b) and were taken as the average value of the measured membrane current in the range of $20 < x$ (μm) < 70 . Similar to the behavior of the membrane current density, the membrane current was roughly proportional to the membrane potential when $0 \leq E_{\text{mem}}$ (mV) ≤ 110 . The membrane current increased less

steeply when the applied potential was increased from 110 to 160 mV, in contrast to the membrane current density. The lack of strict consistency with eq 11 can probably be ascribed to a change in membrane area during the experiments. For example, if the BLM is assumed to be a disk, the radius of the membrane, R_{mem} , can be obtained by inserting $A_{\text{mem}} = \pi R_{\text{mem}}^2$ into eq 11 and by combining the resulting equation with eq 10

$$R_{\text{mem}} = \sqrt{-(4.64 a i_{\text{mem}} / \pi m)} \quad (12)$$

The membrane radius thus obtained is 0.90 ± 0.03 mm (Table 1), which reasonably agrees with observation by optical microscopy. The membrane radii for $E_{\text{mem}} = 60$ and 160 mV were nearly the same but are significantly larger than the membrane radius for $E_{\text{mem}} = 110$ mV. This result suggests that the membrane area increased after the experiment with $E_{\text{mem}} = 110$ mV, corresponding to the change of the membrane position after the experiment, as shown in Figure 7a. Note that the transfer of the supporting electrolyte, which would contribute to the membrane current but not to the tip current, can be excluded as the reason for the lack of strict consistency of the experimental results with eq 11, because in cell 2, the supporting electrolytes in the aqueous phase do not move through the gramicidin pores.^{36,37,44}

CONCLUSIONS

Voltammetric K^+ -selective micropipet electrodes based on valinomycin were fabricated and characterized on the basis of the voltammetric and SECM experiments. The well-defined steady-state responses of the micropipet electrodes agree well with the theory in both experiments. Analysis of an approach curve showed that a tip–substrate distance as close as 115 nm could be achieved with a pipet electrode with a tip radius of 710 nm. This result confirms that submicrometer-scale pipet electrodes, which are

useful for fast kinetic measurements and for high-resolution SECM imaging^{1,2} can be easily fabricated.

The voltammetric K^+ -selective micropipet electrodes were used in the SECM feedback and generation–collection experiments to probe K^+ transfer through gramicidin channels in BLMs. Obviously, these experiments cannot be achieved with conventional microelectrodes that are sensitive only to electrochemically active mediators, indicating an advantage of voltammetric ion-selective micropipet electrodes. Furthermore, in contrast to the potentiometric counterpart, the feedback effect on the steady-state current responses of the voltammetric micropipet electrodes provides information not only about the tip–membrane distance but also about the area of the BLM by simultaneously measuring the membrane current. Voltammetric ion-selective micropipet electrodes have been used previously in SECM experiments with only simple substrates.^{25–27,55} This study clearly shows that the voltammetric ion-selective micropipet electrodes are useful in the SECM studies of IT across BLMs and perhaps even biological membranes.⁵⁶

ACKNOWLEDGMENT

The support of this research by grants from the Robert A. Welch Foundation and the National Science Foundation (CHE 9870762) is gratefully acknowledged. S.A. thanks the Japan Society for the Promotion of Science for a postdoctoral fellowship.

Received for review April 10, 2000. Accepted July 17, 2000.

AC0004207

(55) Selzer, Y.; Mandler, D. *J. Phys. Chem. B* **2000**, *104*, 4903–4910.

(56) Evans, N. J.; Gonsalves, M.; Gray, N. J.; Barker, A. L.; Macpherson, J. V.; Unwin, P. R. *Electrochem. Commun.* **2000**, *2*, 201–206.